Analyst

ROYAL SOCIETY OF CHEMISTRY

CRITICAL REVIEW

View Article Online
View Journal | View Issue

Cite this: *Analyst*, 2020, **145**, 5713

Stimuli-responsive polymer/nanomaterial hybrids for sensing applications

Tong Shu,[a,b] Qiming Shen,[c] Xueji Zhang [a,b] and Michael J. Serpe *[c]

Received 7th April 2020,
Accepted 29th June 2020

DOI: 10.1039/d0an00686f

rsc.li/analyst

Chemical and biological/biochemical sensors are capable of generating readout signals that are proportional to the concentration of specific analytes of interest. Signal sensitivity and limit of detection/quantitation can be enhanced through the use of polymers, nanomaterials, and their hybrids. Of particular interest are stimuli-responsive polymers and nanomaterials due to their ability to change their physical and/or chemical characteristics in response to their environment, and/or in the presence of molecular/biomolecular species of interest. Their individual use for sensing applications have many benefits, although this review focuses on the utility of stimuli-responsive polymer and nanomaterial hybrids. We discuss three main topics: stimuli-responsive nanogels, stimuli-responsive network polymers doped with nanomaterials, and nanoparticles modified with stimuli-responsive polymers.

Introduction

Polymer technology and nanotechnology has proven to be vital to the development of all modern technologies.[1–6] Particularly, rapid developments in these respective fields have led to important advances in the field of micro/nano-electronics, which has allowed for increasing small features to be generated, *e.g.*, features with critical dimensions as small as 7 nm.[7,8] Additionally, research in these respective fields individually have allowed polymer-based nanomaterials to be developed, and of specific interest to this review are hydrogel nanoparticles (nanogels).[9,10] Over the years, nanogels have been synthesized using a variety of approaches, *e.g.*, using emulsions, precipitation, gelation, grinding, and microfluidics.[11] Polymers can also be used to add new and interesting properties to nanomaterials by grafting organic polymers on the surface of inorganic nanoparticles or by incorporating functional nanomaterials into a polymer matrix. Polymers can be grafted onto nanomaterials using grafting to/grafting from techniques,[12–14] while polymer networks can be imbibed with nanomaterials by exploiting various physical/chemical interactions.[3,15,16] This novel class of materials, also known as nanocomposites, can enhance the properties of each of the respective materials on their own, to yield a synergistic effect from the materials to achieve enhanced properties, *e.g.*, mechanical and electrical properties,[17] catalytic performance,[18,19] biocompatibility,[20] stimuli-responsivity.[21] Therefore, a broad range of related topics have emerged in recent decades, including electrospun nanofibers,[22] polymer-based biomaterials,[23,24] layer-by-layer self-assembled polymer films,[25] polymer actuation,[26] drug delivery,[27] imprint lithography,[28] and chemical and biological/biochemical sensors.[29]

Chemical and biological/biochemical sensors are devices or probes that can respond to the presence of an analyte to generate a corresponding signal, *e.g.*, electrical or optical.[30–32] They are widely used in the fields of environmental monitoring (*e.g.*, to detect water contaminants) and human health (*e.g.*, for disease diagnosis, and health monitoring).[33,34] Advances in materials science and engineering have led to great improvements in the performance of chemical and biochemical sensors. For example, hydrogels, molecular imprinted polymers, and conducting polymers, have been developed that yield improved sensitivity, selectivity, and limit of detection/quantitation.[35] Additionally, stimuli-responsive polymers have attracted considerable interest in the field of chemical and biochemical sensors, due to their ability to respond a stimulus (or the presence of an analyte) by changing their physical and/or chemical properties.[36,37] Stimuli include, but are not limited to, temperature,[38] light,[39] and electric and magnetic fields.[40] Furthermore, the stimuli responsivity of polymer-based materials can be enhanced by rationally coupling them with molecular or nanomaterial probes, *e.g.*, fluorophores,[41] metal nanoparticles,[42] and quantum dots.[43] Additionally, polymer-based materials exhibit many appealing properties, including: flexibility/stretchability, transparency, biocompatibility, and

[a]*School of Biomedical Engineering, Health Science Center, Shenzhen University, Shenzhen, Guangdong 518060, China*
[b]*Beijing Key Laboratory for Bioengineering and Sensing Technology, Research Center for Bioengineering and Sensing Technology, School of Chemistry and Biological Engineering, University of Science and Technology Beijing, Beijing 100083, P. R. China*
[c]*Department of Chemistry, University of Alberta, Edmonton, Alberta, Canada T6G 2G2. E-mail: serpe@ualberta.ca; Fax: +1 780 492 8231; Tel: +1 780 492 5778*

inertness to many chemical and physical challenges; these properties make them ideal for myriad applications, *e.g.*, wearable sensors.[44,45] While much has been done with these materials related to chemical and biochemical sensing, recent nanotechnological advances have allowed sensing technology to reach new heights.[46]

Previous reviews on stimuli-responsive polymer/nanomaterial composites have been focused on the applications to shape memory,[47] textiles,[48] and drug delivery.[49] However, reviewing the utility of these materials for sensing applications is not as common. Therefore, this review will focus on highlighting work in this area over the past five years. Specifically, we highlight three types of hybrid materials, *e.g.*, nanogels, stimuli-responsive polymer-based networks combined with nanomaterials and nanomaterials with stimuli-responsive polymer surface coatings, and their use for sensing applications. In each section, we will highlight the role of polymers and nanomaterials on analyte recognition and signal transductions to achieve desirable sensors.

Nanogels

Nanogels are colloidally stable nanoscale hydrogel particles composed of hydrophilic groups that enable them to absorb and retain considerable amounts of water without dissolution.[50,51] The interaction between small molecules and the polymer network can trigger a volume change of the nanogel.[52] By incorporating various recognition moieties into the nanogel network, they can respond to a variety of analytes, which makes them ideal candidates for sensing applications.[52–54] Moreover, the nanogel network can increase the stability of some sensitive recognition moieties and enhance their solubility to allow for sensing in aqueous solutions.[55–57] Compared to macroscale hydrogels, nanogels have many merits. For example, nanogels have a high surface area to volume ratio that improves their binding efficiency to analytes relative to more macroscopic materials. Furthermore, the response time for a volumetric change is proportional to the square of the gel's radius.[58] Therefore, when the size of the hydrogel decreases, the response time likewise decreases. In addition, nanogels are suitable for *in vivo* sensing due to their small size and good biocompatibility.[59] Here, some nanogel-based sensors will be highlighted.

The choice of monomer used to generate nanogels dictates their properties, *e.g.*, certain monomers can render them stimuli-responsive. When synthesizing stimuli-responsive nanogels, it is common to use amine-containing monomers, carboxylic acid-containing monomers, and acrylamide-containing monomers. Amine and carboxylic acid-containing monomers can easily be modified with biomolecules *via* various crosslinking chemistries, which imparts bioresponsivity to the nanogels; these monomers themselves also render the nanogels pH responsive. Acrylamide-containing monomers can render the nanogels temperature responsive, allowing them to change their solvation state with temperature (thermoresponsivity). Furthermore, thermoresponsivity can improve the performance of nanogel-based sensors by altering the microenvironment inside the nanogels, and enhancing fluorescence (for example).[56,60] Herein, we will provide some examples of nanogel-based sensor utilizing these types of monomers.

Amine-containing monomers are widely used for generating nanogels for applications. Monomers with primary amine functional groups can be coupled to carboxylic acid-containing molecules *via* the 1-ethyl-3-(3-dimethylaminopropyl) carbodiimide/*N*-hydroxysuccinimide (EDC/NHS) coupling reaction,[61] which can be used to incorporate fluorescent molecules or biomolecules into nanogels for sensing applications. For example, Li *et al.* constructed a polyacrylamide-based nanogel sensor for the colorimetric measurement of ionizing radiation doses.[62] They copolymerized acrylamide (AAm), *N*-(3-aminopropyl)methacrylamide (APMA), and APMA-modified 5(6)-carboxytetramethylrhodamine (APMA modified-TAMRA), to form poly(AAm-*co*-APMA-*co*-TAMRA) (PAAT) nanogels. Then coumarin-3-carboxylic acid (CCA) was attached to the amino groups of PAAT nanogels *via* an EDC/NHS coupling reaction forming poly-(AAm-*co*-APMA-*co*-TAMRA)/CCA (PAATC) nanogels as shown in Fig. 1. The nanogel sensor had two fluorescent moieties TAMRA and CCA. When exposed to ionizing radiation, the CCA moiety gained a hydroxyl group on its C7 position by reacting with hydroxyl radicals generated from water radiolysis. The resulting 7-hydroxyl-coumarin-3-carboxylic acid (7-OH-CCA) emitted strong blue light (λ_{em} = 450 nm) under UV excitation. On the contrary, the TAMRA moiety emitted red fluorescence light (λ_{em} = 580 nm) under UV light, and the intensity was not affected by ionizing radiation doses. Therefore, a ratiometric strategy could be applied to this nanogel sensor. By measuring the fluorescence intensity ratio of nanogels at 450 and 580 nm (I_{450}/I_{580}), the ionizing radiation dose could be determined. The sensor provided good linearity over a range of X-ray doses (0–20 Gy) with a LOD of 0.1 Gy and the maximum error of standard deviation of 4.2%.

In another example, Haag and coworkers synthesized dendritic polyglycerol nanogels (dPG-NGs) as pH sensors in the hair follicle, which can guide the development of skin pH-responsive nanocarriers for drug delivery.[63] Dendritic polyglycerol amine (dPG-NH_2) was first modified with pH-sensitive indodicarbocyanine dye (pH-IDCC) and a control dye (indocarbocyanine dye: ICC) *via* an *N*-hydroxysuccinimide (NHS) ester coupling. The dye-labeled dPG-amines were thiolated and crosslinked with dPG-acrylate *via* thiol-Michael reaction, generating dPG-NGs as shown in Fig. 2. The fluorescence intensity of pH-IDCC dye changed as a function of pH while the fluorescence intensity of ICC dye was not affected regardless of pH. The nanogel sensor could penetrate the skin and measure the pH in the hair follicle. By plotting the fluorescence intensity ratio of pH-IDCC over ICC, the author observed a good linear relationship with increasing pH within the physiologically important pH range 5.5 to 7.5.

In addition to utilizing the amine group to couple to carboxyl group-containing molecules, nanogels with protonated

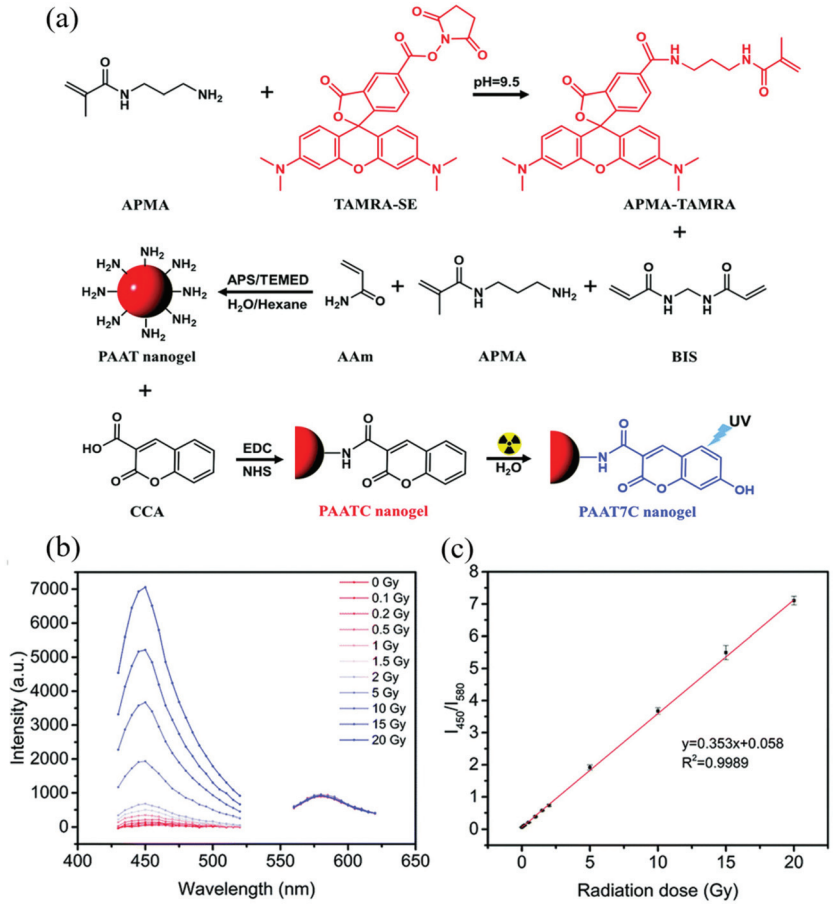

Fig. 1 (a) Synthetic route and the mechanism of PAATC nanogels for sensing ionizing radiation doses. (b) Fluorescence emission spectra at 400 nm and 530 nm under various ionizing radiation doses. (c) Fluorescence ratio (I_{450}/I_{580}) of the PAATC nanogels after exposure to X-rays in the range of 0–20 Gy. Reprinted (adapted) with permission from ref. 62. Copyright (2019) Royal Society of Chemistry.

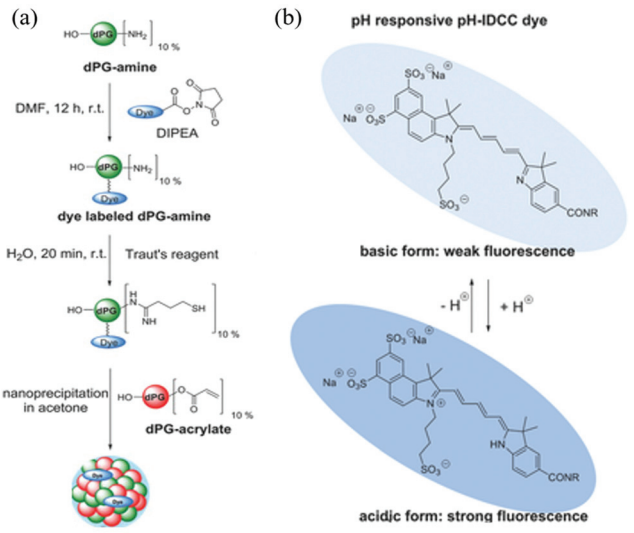

Fig. 2 (a) Synthetic route for generating the functional nanogels, and (b) the chemical structures of the dye (pH-IDCC) in its protonated and deprotonated forms. Reprinted (adapted) with permission from ref. 63. Copyright (2017) Wiley Online Library.

amine groups can interact with anions, resulting in the neutralization of the amine's positive charges and shrinkage of the nanogels. Recently, Zhang *et al.* synthesized a poly(*N*-isopropylacrylamide)-*co*-*N*-(3-aminopropyl) methacrylamide hydrochloride (pNIPAm-*co*-APMAH) micro/nanogel for the detection of mouse immunoglobulin G (IgG).[64] Mouse IgG was captured by magnetic microspheres modified goat anti-mouse IgG (GAM@M). An excess amount of alkaline phosphatase-modified goat anti-mouse IgG (AP-GAM) was added to mouse IgG. After the application of a magnetic field, the excess free AP-GAM was isolated and used to degrade a phosphate-containing polymer to release phosphate anions. The pNIPAm-*co*-APMAH micro/nanogel interacted with the phosphate anions and resulted in the deswelling of the nanogel. The shrinkage of the nanogel was monitored by an etalon device. The sensor had the ability to detect low concentrations of mouse IgG down to the nanomolar range. In a similar example, Islam *et al.* utilized pNIPAm-*co*-APMAH micro/nanogels for the detection of single-stranded DNA (ssDNA).[65] The target ssDNA was selectively captured and separated by magnetic microparticles modified with the complimentary DNA

strands. After separation, the magnetic particles were heated to release the target DNA. The target DNA had multiple negative charges, which could neutralize the positive charges of pNIPAm-*co*-APMAH micro/nanogel. The corresponding shrinkage of nanogels was quantified by a pNIPAm-*co*-APMAH micro/nanogel-based etalon sensor. The sensor was able to detect the concentration of DNA down to the micromolar in range without any amplification or preconcentration of the sample.

Carboxylic acid-containing monomers have also been shown to have great utility for sensing applications. Carboxylic acids are weak acids, with their ionization extent being dependent on pH. Therefore, nanogels with carboxylic acid monomers (*e.g.* acrylic acid and methacrylic acid) are commonly used for pH sensing. Compared to commonly used amperometric or potentiometric devices, nanogel-based pH sensors do not require constant re-calibration and they have low manufacturing cost.[66] Furthermore, their good biocompatibility allows nanogels to be used in the human body to measure intracellular pH.[53,59] Recently, Zhu *et al.* reported an non-radiative resonance energy transfer (NRET)-based nanogel probe for pH sensing.[67] The authors fabricated the nanogel probe by copolymerizing methylmethacrylate (MMA), methacrylic acid (MAA), and ethylene glycol dimethacrylate (EGDMA) with two NRET fluorophore pairs, donor (9-phenanthryl)methylmethacrylate (Ph) and acceptor (9-anthryl)methacrylate (An). The carboxylic acid groups from MAA were deprotonated as pH increased to form carboxylate groups, resulting in charge repulsion and the swelling of nanogels. The swelling process increased the distance between the donor and acceptor, which hindered the NRET process as shown in Fig. 3. As a result, the fluorescence intensity ratio (I_{Ph}/I_{An}) increased as pH increased. Such nanogel probes have exhibited desirable potential as a versatile ratiometric fluorescent platform for sensing pH.

Like amine-containing monomers, carboxylic acid-containing monomers can also be used to conjugate to various biomolecules such as enzymes and antibodies, which allows the corresponding nanogel to respond to a variety of biologically-relevant analytes. For example, hydrogen peroxide (H_2O_2) is one of the most important reactive oxygen species (ROS) and is a crucial signaling molecule in the regulation of many biological processes.[68,69] Though H_2O_2 plays an important role in cellular signal transduction, overexpressed H_2O_2 can severely damage cells and lead to several diseases such as cancer, cardiovascular disorders, and neurodegeneration. Ghimire *et al.* reported an enzymatic H_2O_2 electrochemical biosensor utilizing met-hemoglobin (Hb) coupled poly(acrylic acid) (Hb-PAA) nanogel-based bioelectrode.[55] In the presence of H_2O_2, the Fe^{2+} in the heme protein of Hb was oxidized to form Fe^{3+}, and the concentration of H_2O_2 could be determined by amperometry. The resulting nanogels possessed high thermal stability and could withstand exposure to high temperature (122 °C) without loss of Hb structure or its peroxidase-like activity. The nanogel-based electrochemical sensor exhibited an excellent detection limit of 0.5 μM H_2O_2. In another example, Yang *et al.* developed a bioresponsive nanogel for the analysis of multivalent protein binding (MPB).[70] The authors synthesized pNIPAm-*co*-AAc nanogels that were conjugated to PD-1, biocytin, or protein A through EDC/NHS coupling reaction. The PD-1 antibody formed a type of MPB by complexing with PD-1 protein and protein A, which enhanced the surface plasmon resonance (SPR) signal by at least 3 times compared to the monovalent SPR analysis. Using MPB-based SPR analysis, the authors were able to detect the PD-1 antibody down to a level of 10 nM.

Temperature responsive monomers have been used extensively to generate nanogels, and used for a variety of sensing applications. While there are a variety of temperature-responsive monomers such as *N*-vinylcaprolactam (NVCL) and 2-(2-methoxyethoxy)ethylmethacrylate (MEO2MA), *N*-isopropylacrylamide (NIPAm) is by far the most extensively studied.[71] PNIPAm exhibits a lower critical solution temperature (LCST) at 32 °C. At that temperature, the pNIPAm chains transition from a random coil to a globular conformation, resulting in the change of its hydrophobicity. Therefore, pNIPAm-based nanogel can be used as temperature sensors.[72,73]

In addition to temperature sensing, temperature-responsive monomers can enhance the sensor performance by changing the microenvironment inside the nanogels. For example, Liu and coworkers developed a nanogel-based fluorescent sensor for Hg^{2+} detection.[56] The thermoresponsive nanogel was prepared by emulsion polymerization of NIPAm and a Hg^{2+} reactive fluorescent 1,8-naphthalimide-based monomer (NPTUA).

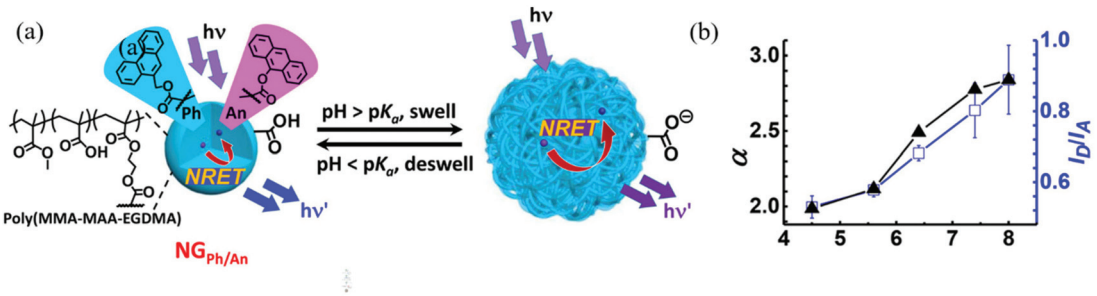

Fig. 3 (a) Schematic depicting the sensing mechanism of pH-responsive nanogel probes (NGPh/An). (b) Variation of the average linear swelling ratio (α) and I_D/I_A with pH for DX NG(NGPh/An). Reprinted (adapted) with permission from ref. 67. Copyright (2017) American Chemical Society.

In the presence of Hg^{2+}, the thiourea moieties of NPTUA were converted into imidazoline moieties. The transformation reduced the fluorescence intensity at 528 nm and created a new emission peak at 482 nm. A ratiometric fluorescent sensor for Hg^{2+} could be fabricated based on the property of NPTUA. The sensor provided good linearity over the Hg^{2+} concentration ranging from 0–10 nM with a detection limit of 5.1 nM. The pNIPAm nanogel enhanced the water solubility of NPTUA, so the sensor could be applied in various aqueous solutions. In addition, the thermoresponsive pNIPAm nanogels collapsed at high temperature and created a hydrophobic microenvironment inside the nanogels, which significantly improved the sensitivity. Chromium ions are responsible for regulating several biological processes such as accelerating insulin action.[74] However, a high concentration of Cr^{3+} increases the risks of DNA dysfunction, diabetes, and autoimmune diseases.[75] In another example, Yao and coworkers developed a fluorescent nanogel sensor for Cr^{3+} detection.[60] NIPAm copolymerized with rhodamine B urea derivatives (RhBUA), generating p(NIPAM-*co*-RhBUA) nanogels. RhBUA could specifically bind to Cr^{3+}, inducing ring-opening of spirolactam moieties. The conformational change caused the non-fluorescent RhBUA to emit light at 580 nm. The intensity of the resultant fluorescence was related to Cr^{3+} concentration, and the detection limit was calculated to be 2.2×10^{-7} M. Compared to other ions, the sensor showed high selectivity towards Cr^{3+}. Furthermore, the sensor exhibited enhanced performance at elevated temperature. That was ascribed to the larger quantum yields of RhBUA in more hydrophobic nanogel microenvironment as well as the higher recognition probability between Cr^{3+} and RhBUA in a collapsed nanogel.

Stimuli-responsive polymer-based networks combined with nanomaterials

Stimuli-responsive polymer-based networks are linear or branch polymers with stimuli-responsive groups that are chemically or physically crosslinked into a three-dimensional (3D) network.[52,76,77] The porous structure of the 3D polymer matrix not only allows small molecules to be transported, but can also be used to contain inorganic nanomaterials with various structures from 0D nanoparticles (*e.g.*, carbon dots[78]), to 1D nanorods (*e.g.*, Au nanorods[79]) and nanofibers (*e.g.*, silicon nanowire[80]) to 2D nanosheets (*e.g.*, MnO_2 nanosheets[81]).[82] With proper design and trials, the obtained nanocomposites generally can exhibit improved properties compared to their counterparts, or novel synergistic functions, *e.g.*, sensing.[83] The sensing capacities of such nanocomposites mostly are based on the efficiency of signal recognition and transduction. Environmental stimuli, *e.g.*, temperature, pH, or ionic content can cause a volume/size change of polymers, which successively changes the chemical/physical properties of embedded nanomaterials, thus exhibiting, for example, an enhancement of the plasmonic signal[84] or the photoluminescence signal.[85]

Noble metal nanoparticles received much attention due to their unique optical and electrical properties as well as good stability. The most widely used method to incorporate them into polymers is *via in situ* reduction after enriching with their oxidized precursors. The Serpe group reported a microgel-based optical device (etalon) for H_2O_2 sensing.[86] Etalons were constructed by sandwiching poly(*N*-isopropylacrylamide-*co*-acrylic acid) (p(NIPAm-*co*-AAc)) micro/nanogel between two Au layers. Then, Ag nanoparticles (AgNPs) were generated in etalons *via* their *in situ* reduction with $NaBH_4$ as shown in Fig. 4. The etalons allowed light with certain wavelengths to be reflected due to constructive and destructive interference in the micro/nanogel-based cavity, and the reflected wavelength was dependent on the size of micro/nanogel particles.[87,88] In the presence of H_2O_2, AgNPs were oxidized and form Ag^+, resulting in the swelling of the gel layer. The reflectance peak shifted to higher wavelength and the reflectance intensity increased due to the increase in diameter of the nano/microgels and less absorption from AgNPs. The sensor showed good linearity within the H_2O_2 concentration ranging from 0.5–6 mM.

Polymer brushes, which are bound on a common surface, to some extent, can be viewed as network polymeric matrix. As shown in Fig. 5, Chen *et al.* prepared a humidity-responsive plasmonic nanosensor by functionalizing a Ag film with poly-

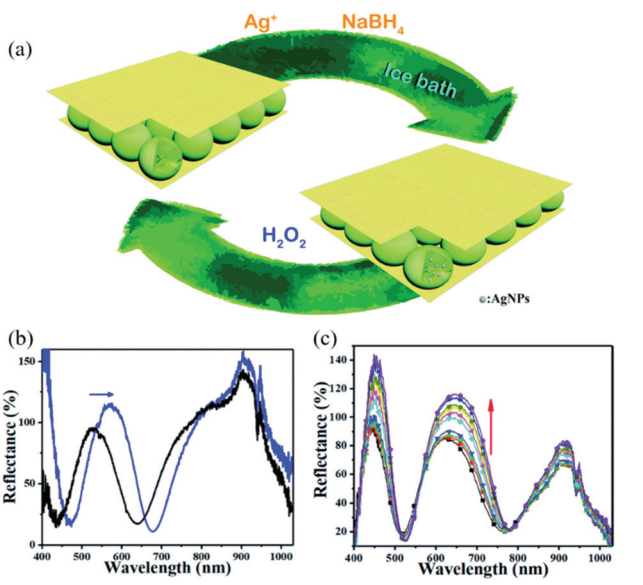

Fig. 4 (a) Schematic illustration of the *in situ* fabrication method of AgNPs@pNIPAm-*co*-AAc hybrid microgels-based etalon and response mechanism of the etalon. (b) Reflectance spectra of etalons with AgNPs upon exposure to 10 mM H_2O_2 at pH 3.0. The blue arrows show the direction of the peak shift. (c) Reflectance spectra of AgNPs-loaded etalon upon exposure to various concentrations of H_2O_2 at pH 7.0 from 0.5 (bottom) to 10 mM (top); the direction of the peak shift is indicated by the red arrow. Reprinted (adapted) with permission from ref. 38. Copyright (2018) Royal Society of Chemistry.

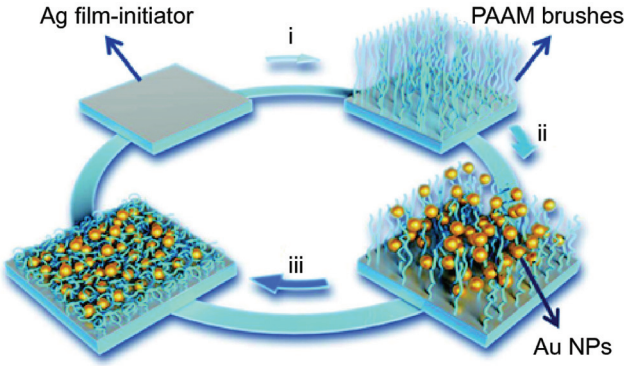

Fig. 5 Schematic illustration of the fabrication of pAAm brushes on Ag film and immobilization of AuNPs. Reproduced (adapted) with permission from ref. 89. Copyright (2018) Springer Nature.

acrylamide (pAAm) brushes *via* surface initiated-atom transfer radical polymerization (SI-ATRP) (step i), where Au nanoparticles (AuNPs) were subsequently incorporated through assembly (step ii), and lastly storing the resultant vacuum-dried film under nitrogen atmosphere (step iii).[89] When the relative humidity increased, the pAAm brushes swelled and thus stretched the nano-gap between the closely spaced AuNPs, and between AuNPs and the Ag film, resulting in noticeable decrease of plasmonic hotspots and SERS signals using 4-mercaptopyridine (4-Mpy) as a molecular probe. The optical changes of the nanocomposite could be reversibly tuned by relative humidity and the resulting relative humidity sensors was shown to be stable for at least two months.

Metal oxide nanoparticles exhibit unique chemical, mechanical, electrical and optical properties due to nanoscale-induced high surface reactivity.[90] Their ultra-small size also allows them to interact in a unique manner with biomolecules and thus facilitates their entrance into the inner cellular microenvironments.[91] Wu *et al.* developed a glucose sensor based on fluorescent ZnO@poly(*N*-isopropylacrylamide-acrylamide-2-aminomethyl-5-fluorophenylboronic acid) (ZnO@p(NIPAm-AAm-FPBA)) nanocomposites.[92] ZnO@p(NIPAm-AAm-AA) that was synthesized by free radical polymerization. Subsequently, a glucose recognition molecule FPBA was coupled to the carboxyl groups of the nanogel *via* EDC coupling reaction. The FPBA moieties captured glucose molecules in solution and resulted in the swelling of the nanogel. The swelling of the nanogel may hinder the access of the excitation light to the fluorescent ZnO. Therefore, the glucose-induced swelling could be converted into a change in fluorescence signal. A good linear relationship was shown between the reciprocal fluorescence intensity and glucose concentrations with a detection limit of 1.7 mg dL^{-1}. Furthermore, the sensor exhibited good selectivity towards glucose in human blood serum samples.

Nanosheets, as an emerging class of nanomaterials including graphenic carbon materials and transition-metal oxide nanosheets with planar topography, exhibit unique properties including high specific surface area and robust physicochemical properties.[93] Zhou *et al.* hybridized graphene oxide (GO), and Hb into temperature-responsive block co-polymer poly(*N*-isopropylacrylamide)-*b*-poly(2-acrylamidoethyl benzoate) (pNIPAm-*b*-PAAE), to prepare a temperature-responsive biosensing film.[94] The film was modified on a glassy carbon electrode (GCE), providing a favorable micro-environment for Hb to facilitate the electron transfer to the GCE. The pNIPAm-*b*-PAAE/GO/Hb (PGH) film exhibited intrinsic electro-catalytic activity toward H_2O_2. The performance of the sensing film could be controlled by temperature, as a result of temperature-dependent phase transition of pNIPAm-bPAAE and cooperative effect of GO. Good linear detection showed in the concentration range from 0.1 to 3.7 μmol L^{-1} when operated at above 32 °C, while the sensitivity decreased to 0.2 μmol L^{-1} at below 30 °C.

Metal nanoclusters (<2 nm) consisting of several to hundreds of noble metal atoms possess intriguing fluorescent properties, *e.g.*, stability under irradiation, a large Stokes shift and size-dependent excitation and emission spectra, making them suitable for fluorescence analytical applications.[95,96] As shown in Fig. 6, Gou *et al.* loaded Cu nanoclusters (CuNCs) and $CaCO_3$ nanoparticles into alginate to prepare pH-responsive luminescent nanocomposites.[97] In these hybridized systems, CuNCs with aggregation-induced emission enhancement features acted as a fluorophore probe for gelation, while $CaCO_3$ nanoparticles responded to pH by releasing Ca^{2+}, which could trigger gelation of alginate. Specifically, decreased solution pH dissolved the $CaCO_3$ nanoparticles and yielded free Ca^{2+}, which was able to crosslink the alginate chains into gel networks. Meanwhile, the emissive intensity of CuNCs was dramatically enhanced, assigned to the Ca^{2+}-induced enhancement and gelation-induced enhancement, synergistically. Their potential application was further expanded as a sensor for glucose by introducing glucose oxidase, which could recognize glucose and decrease the solution pH. In another example, Jianhua Lü *et al.* decorated temperature-responsive copolymers p(NIPAm-*co*-MQ) with luminescent Ag nanoclusters (AgNCs) to fabricate fluorescent pH-responsive nanocomposites.[98] p(NIPAm-*co*-MQ) consisted of two components, NIPAm as the thermoresponsive units and 5-(2-methacryloylethyloxymethyl)-8-quinolinol (MQ) as anchoring groups. The obtained nanocomposites exhibited different morphologies from spherical to chain structures. When the temperature was increased, the fluorescence intensity of the AgNCs was reversibly enhanced. They also found that the nanocomposites exhibited pH-dependent fluorescence properties over the pH range of 3.04–5.25. As the solution pH decreased, the fluorescence intensity of AgNCs reversibly decreased. In yet another example, Shen *et al.* prepared stimuli-sensitive nanocomposites with AgNCs by loading them into p(NIPAm-*co*-AAc) microgels.[99] The red-emissive nanocomposites showed high sensitivity and selectivity towards Cr^{4+} in aqueous solutions. Structurally, the p(NIPAm-*co*-AAc) microgels acted as templates for AgNCs and exhibited thermoresponsivity, while AgNCs endowed excellent photoluminescent properties to the nanocomposites. AgNCs were formed *in situ* by photoreduction of

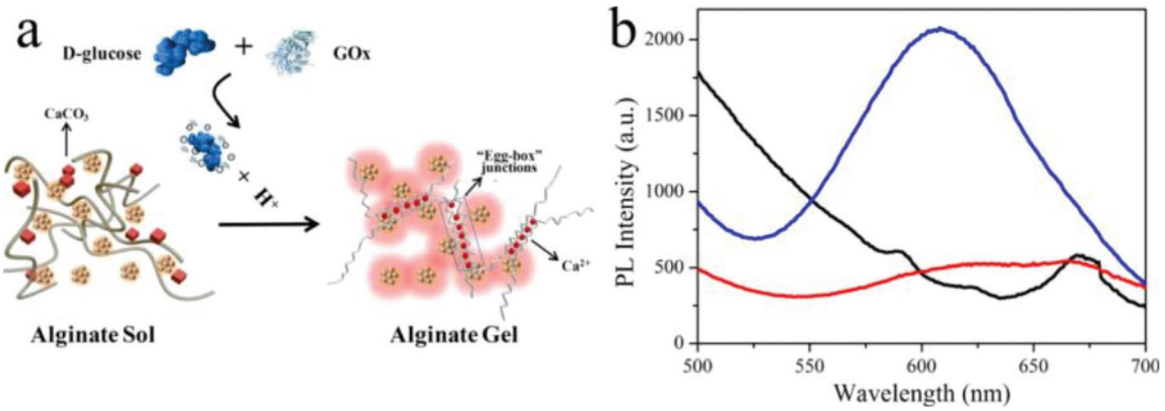

Fig. 6 (a) Schematic illustration of the glucose sensor using hybrid CuNC-alginate; (b) PL spectra of Cu NCs (red), Cu NCs + alginate (black), and CuNCs + alginate + glucose + GOx (blue). Reprinted (adapted) with permission from ref. 97. Copyright (2019) American Chemical Society.

Ag^+. The fluorescent nanocomposites exhibited a linear and reversible response from 2 to 85 °C and displayed high fluorescence quenching for the sensitive and selective detection of Cr^{4+} rather than Cr^{3+}.

Nanomaterials with polymer surface modification

Modification of nanomaterials with polymer can serve many purposes, *e.g.*, protection from aggregation,[42] and modulation of their interaction with environment.[100] For sensing applications, analytes generally first interact with polymers on the surface and trigger their response, which can result in a change of the physiochemical properties of the nanomaterial nanomaterials, and yield a detectable response.[37] In short, responsive polymers play the role of the recognition unit, while the nanomaterials are transduction elements in such sensing system.

2D planar nanomaterials, *e.g.*, graphene oxides (GOs), exhibit beneficial properties for sensing applications.[101] The specific sp^2 domains of GOs endow them with broad and strong absorption in the visible region with the ability to be readily modified. Thus, they are often used as quenchers in the fabrication of fluorescent sensors.[46] Kim's group developed a highly efficient and stable GO-based optical pH sensor with quantum dots (QDs).[102] The key to the function of this sensing platform is the rational use of pH-responsive polymers. The photoluminescent emission of the blue and orange color-emitting QDs (BQDs and OQDs) in MQD-GO can be controlled independently by using different pH-responsive linkers of poly(acrylic acid) (PAA) (pK_a = 4.5) and poly(2-vinylpyridine) (P2VP) (pK_a = 3.0) that can tune the efficiencies of Förster resonance energy transfer from the BQDs to the GO and from the OQDs to the GO, respectively. As a result, the color of MQD-GO changes from orange to near-white to blue over a wide range of pH values. Interestingly, although GO can quench fluorescence, it is also itself fluorescent, due to electron–hole pairs in localized electronic states originating from various possible configurations. In another example from Kim's group (as shown in Fig. 7), they integrated graphene quantum dots (GQDs) with coumarin modified stimuli-responsive block copolymers to generate a multianalyte sensing system.[102] This multi-responsive platform was constructed simply by grafting blue-emitting, temperature-responsive block copolymers onto green-emitting GQDs that provides a luminescent response to pH changes.

Among noble metal nanoparticles, AuNPs are mostly used for sensing applications due to their biocompatibility, their optical and electronic properties, and their relatively simple production and modification.[103] AuNPs exhibit SPR, which leads their solutions to exhibit various colors.[104] The electron oscillation of nanoparticles is largely affected by their size and the dielectric constant of their environment. This change of the oscillation frequency results in a color change of the AuNPs observable with the naked eye, laying the foundation of AuNPs-based colorimetric sensors. In one example, Ma *et al.* generated CO_2 colorimetric sensors by the *in situ* preparation of CO_2-responsive poly(*N*-(3-amidino)-aniline) (PNAAN)-coated AuNPs.[105] In this synthesis, $HAuCl_4$ oxidized and polymerized the monomer *N*-(3-amidino)-aniline (NAAN) into PNAAN, while $HAuCl_4$ itself was reduced to form AuNPs stabilized by PNAAN. The dissolved CO_2 could protonate the amidine groups of PNAAN, resulting in the swelling of and then the detachment of PNAAN from the AuNPs. This finally led to AuNPs aggregation and a concomitant color change. The strategies based on aggregation-induced color changes are widely used in AuNPs-based sensors. In another example, Maji *et al.* covalently bound thermoresponsive pNIPAm onto citrate-stabilized AuNPs, adding an extra polymer stabilizer in addition to charge stabilization.[106] Due to the dual stabilization mechanism, only when both stimuli were applied did the color of the AuNP solution change. This dual-stimuli triggered response could be further exploited for the development

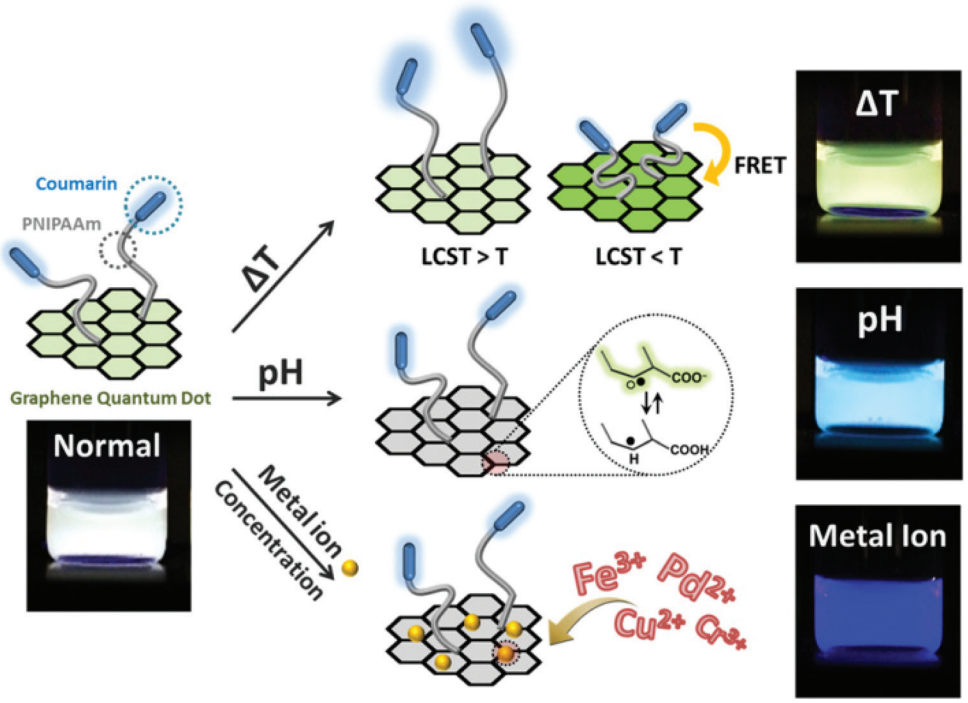

Fig. 7 Structure of block copolymer-grafted graphene quantum dots (bcp-GQDs) and their sensing behavior. Reprinted (adapted) with permission from ref. 102. Copyright (2015) American Chemical Society.

of temperature and salt sensors, respectively. The sensing regime for one of them can be tuned by changing the condition of the other.

The polymer ligands of nanomaterials also can be used to load signal molecules. As shown in Fig. 8, Bodelón *et al.* fabricated highly stable surface-enhanced resonance Raman scattering (SERRS)-encoded colloids for the identification of cellular protein expression. SERRS is another useful property of AuNPs.[107] AuNPs were coated with a pNIPAm network, where Raman active dyes can readily be encapsulated. A further layer-by-layer polyelectrolyte coating on the outer surface of the particles prevented the leakage of and provided a reactive surface for covalent conjugation with antibodies. With the loading of different SERRS tags, the hybrid particles could simultaneously detect and image three tumor-associated surface biomarkers: epidermal growth factor receptor (EGFR), epithelial cell adhesion molecule (EpCAM), and homing cell adhesion molecule (CD44) by SERRS spectroscopy. On the other hand, the surface of AuNPs is readily grafted by polymer brushes. In one example, Wang *et al.* reported a sandwich type electrochemical immunosensor for simultaneous and high sensitive detection of two tumor markers.[108] They incorporated a functional polymer brush, poly(acrylonitrile-*g*-glycidyl methacrylate), onto the surface of AuNPs. The side chains of polymers were loaded with electrochemical mediators, while the ends of the polymer chains were conjugated with antibody. This electrochemical immunosensor exhibited excellent detection limits at 10 pg mL^{-1} for both prostate specific antigen (PSA) and a-fetoprotein (AFP).

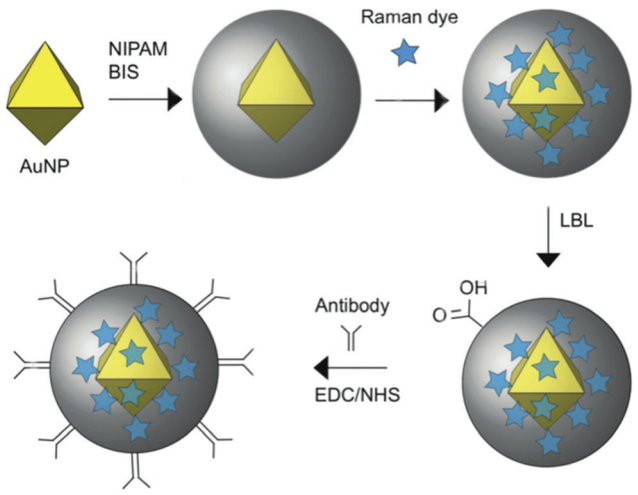

Fig. 8 Schematic representation of the preparation of Au@pNIPAM SERRS-encoded tags. Reprinted (adapted) with permission from ref. 107. Copyright (2015) Wiley Online Library.

The high specific surface area of nanomaterials also provides abundant sites for polymer growth. Kong's group has been dedicated to developing polymerization-based signal amplification strategies. In one example, they modified magnetic nanoparticles (MNPs) with hairpin DNA probes (pDNA) labelled with 5′ thiol and 3′ azide group. An ultrasensitive fluorescent HTLV-II DNA detection strategy was developed based on MNPs and atom transfer radical polymerization (ATRP)

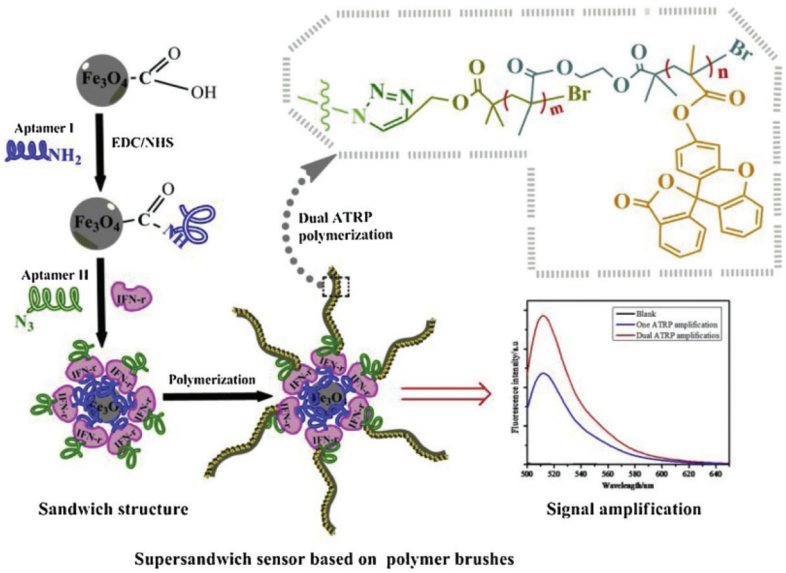

Fig. 9 Schematic illustration of ultrasensitive aptamer fluorometric IFN-γ detection by dual ATRP amplification. Reprinted (adapted) with permission from ref. 110. Copyright (2019) Elservier.

amplification.[109] In the presence of target DNAs (tDNA), hairpin pDNA hybridized with tDNA to form double stranded DNA. Its azide group was thus away from the MNP surface. Subsequently, bromo ATRP initiators were modified on the 3′ end of the pDNA by a Cu(I)-catalyzed alkyne–azide cycloaddition (CuAAC). Then, large numbers of fluorophore monomers, 9-anthracenylmethyl methacrylate, could thus be labelled on the MNPs surface, resulting in considerable amplification of the fluorescence signal. With this method, they successfully developed an ultrasensitive biosensor for the DNA of human T-lymphotropic virus type II (HTLV-II), a crucial retrovirus that is closely associated with a variety of human diseases. Moreover, this strategy was also applicable for constructing aptasensors. Kong's group incorporated two aptamers as protein probes. As shown in Fig. 9, one aptamer probe was attached onto MNPs *via* surface self-assembly, while the other was linked with azide groups. Then, bromo ATRP initiators were introduced on the end of the aptamer *via* click reaction. Subsequently, the ATRP reaction was initiated using the bromo monomers. The resulting bromo polymers were further used as the initiators to trigger a second ATRP reaction based on fluorescein-*o*-acrylate.[110] When exposed to target proteins, an "aptamer/protein/aptamer–polymer" super-sandwich structure would form on the modified MNPs, resulting in accumulation of large numbers of fluorescence signal monomers. Thus, an ultrasensitive aptamer fluorometric method for gamma-interferon (IFN-γ) protein assay could be fabricated.

Conclusion and outlook

We have reviewed a number of examples of responsive polymer/nanomaterial hybrids, and their use for chemical and biological/biochemical sensing. As highlighted in the numerous examples included in this review, the stimuli-responsive polymer is typically responsible for analyte recognition, while the nanomaterial provides a route for signal transduction due to their unique optical, electrical and magnetic properties. By combining these materials, sensing technologies with improved properties can be achieved. While significant advances have been made to generate sensors in laboratory, these technologies are still far from commercialization and benefiting the "real world". This is mostly due to the fact that these materials have difficulty operating in complex media, *e.g.*, blood. The complexity introduced by biosystems might be systematically solved using a precise integrated sensing platform, which is logically structured with functional modules, for example, antipollution coatings, analyte enriching units, and biocompatible components. Thus, more integration and "intelligence" in the microworld should be a future pursuit in the sensing field using stimuli-responsive polymer technology and nanotechnology. On the other hand, we are now entering the age of the "internet of things", due to the high pace development of artificial intelligence (AI) and "5G" wireless technologies. We believe that interdisciplinary collaborations, *e.g.*, microelectronic engineering providing programmable hybridization of micro/nano-structures, wireless transmission for easy signal output *e.g.*, from human body, data sciences and AI, will push chemical and biological/biochemical sensing to new heights with more novel and exciting opportunities and challenges.

Conflicts of interest

The authors declare no conflict of interest.

Acknowledgements

MJS acknowledges funding from the University of Alberta (the Department of Chemistry and the Faculty of Science), the Natural Sciences and Engineering Research Council of Canada (NSERC), the Canada Foundation for Innovation (CFI), the Alberta Advanced Education & Technology Small Equipment Grants Program (AET/SEGP), Grand Challenges Canada. TS acknowledges support from the National Natural Science Foundation of China (21904011, 21890742) and the Fundamental Research Funds for the Central Universities (FRF-TP-19-010A3, FRF-BR-18-009B). MJS and TS acknowledge the National Natural Science Foundation of China (21750110449).

References

1 O. Rötting, W. Röpke, H. Becker and C. Gärtner, *Microsyst. Technol.*, 2002, **8**, 32–36.
2 H. Becker and C. Gärtner, *Anal. Bioanal. Chem.*, 2008, **390**, 89–111.
3 H. Zou, S. Wu and J. Shen, *Chem. Rev.*, 2008, **108**, 3893–3957.
4 N. Kamaly, B. Yameen, J. Wu and O. C. Farokhzad, *Chem. Rev.*, 2016, **116**, 2602–2663.
5 K. E. Sapsford, W. R. Algar, L. Berti, K. B. Gemmill, B. J. Casey, E. Oh, M. H. Stewart and I. L. Medintz, *Chem. Rev.*, 2013, **113**, 1904–2074.
6 L. Cheng, C. Wang, L. Feng, K. Yang and Z. Liu, *Chem. Rev.*, 2014, **114**, 10869–10939.
7 C. Qiu, Z. Zhang, M. Xiao, Y. Yang, D. Zhong and L.-M. Peng, *Science*, 2017, **355**, 271–276.
8 D. R. Paul and L. M. Robeson, *Polymer*, 2008, **49**, 3187–3204.
9 X. Zhang, S. Malhotra, M. Molina and R. Haag, *Chem. Soc. Rev.*, 2015, **44**, 1948–1973.
10 M. V. Priya, M. Sabitha and R. Jayakumar, *Carbohydr. Polym.*, 2016, **136**, 609–617.
11 H. M. Shewan and J. R. Stokes, *J. Food Eng.*, 2013, **119**, 781–792.
12 S. Kango, S. Kalia, A. Celli, J. Njuguna, Y. Habibi and R. Kumar, *Prog. Polym. Sci.*, 2013, **38**, 1232–1261.
13 C. M. Homenick, G. Lawson and A. Adronov, *Polym. Rev.*, 2007, **47**, 265–290.
14 R. M. Bielecki, P. Doll and N. D. Spencer, *Tribol. Lett.*, 2013, **49**, 273–280.
15 Z. H. Farooqi, S. R. Khan and R. Begum, *Mater. Sci. Technol.*, 2016, **33**, 129–137.
16 L. Voorhaar and R. Hoogenboom, *Chem. Soc. Rev.*, 2016, **45**, 4013–4031.
17 Y.-T. Liu, M. Dang, X.-M. Xie, Z.-F. Wang and X.-Y. Ye, *J. Mater. Chem.*, 2011, **21**, 18723–18729.
18 K. C. Chang, C. H. Hsu, H. I. Lu, W. F. Ji, C. H. Chang, W. Y. Li, T. L. Chuang, J. M. Yeh, W. R. Liu and M. H. Tsai, *eXPRESS Polym. Lett.*, 2014, **8**, 243–255.
19 S. A. Nikolaev and V. V. Smirnov, *Catal. Today*, 2009, **147**, S336–S341.
20 I.-Y. Jeon and J.-B. Baek, *Materials*, 2010, **3**, 3654–3674.
21 H. Lu, Y. Yao, W. M. Huang, J. Leng and D. Hui, *Composites, Part B*, 2014, **62**, 256–261.
22 J. Xue, T. Wu, Y. Dai and Y. Xia, *Chem. Rev.*, 2019, **119**, 5298–5415.
23 W. L. A. Brooks and B. S. Sumerlin, *Chem. Rev.*, 2016, **116**, 1375–1397.
24 I. Cobo, M. Li, B. S. Sumerlin and S. Perrier, *Nat. Mater.*, 2015, **14**, 143–159.
25 J. Borges and J. F. Mano, *Chem. Rev.*, 2014, **114**, 8883–8942.
26 L. Hu, Y. Wan, Q. Zhang and M. J. Serpe, *Adv. Funct. Mater.*, 2019, **30**, 1903471.
27 Y. Gao, M. Wei, X. Li, W. Xu, A. Ahiabu, J. Perdiz, Z. Liu and M. J. Serpe, *Macromol. Res.*, 2017, **25**, 513–527.
28 M. C. Traub, W. Longsine and V. N. Truskett, *Annu. Rev. Chem. Biomol. Eng.*, 2016, **7**, 583–604.
29 M. J. Whitcombe, I. Chianella, L. Larcombe, S. A. Piletsky, J. Noble, R. Porter and A. Horgan, *Chem. Soc. Rev.*, 2011, **40**, 1547–1571.
30 K. L. Hamner, C. M. Alexander, K. Coopersmith, D. Reishofer, C. Provenza and M. M. Maye, *ACS Nano*, 2013, **7**, 7011–7020.
31 L. Ionov, *J. Mater. Chem.*, 2010, **20**, 3382–3390.
32 H. Meng and J. Hu, *J. Intell. Mater. Syst. Struct.*, 2010, **21**, 859–885.
33 M. Mayer and A. J. Baeumner, *Chem. Rev.*, 2019, **119**, 7996–8027.
34 Z. He, T. Shu, L. Su and X. Zhang, *Molecules*, 2019, **24**, 3045.
35 W. S. P. Carvalho, M. Wei, N. Ikpo, Y. Gao and M. J. Serpe, *Anal. Chem.*, 2018, **90**, 459–479.
36 W. Lu, X. X. Le, J. W. Zhang, Y. J. Huang and T. Chen, *Chem. Soc. Rev.*, 2017, **46**, 1284–1294.
37 M. Wei, Y. Gao, X. Li and M. J. Serpe, *Polym. Chem.*, 2017, **8**, 127–143.
38 T. Shu, Q. Shen, L. Su, X. Zhang and M. J. Serpe, *ACS Appl. Nano Mater.*, 2018, **1**, 1776–1783.
39 Q. M. Zhang, W. Wang, Y.-Q. Su, E. J. M. Hensen and M. J. Serpe, *Chem. Mater.*, 2016, **28**, 259–265.
40 W. L. Zhang and H. J. Choi, *Polymers*, 2014, **6**, 2803–2818.
41 B. Saha, K. Bauri, A. Bag, P. K. Ghorai and P. De, *Polym. Chem.*, 2016, **7**, 6895–6900.
42 D.-M. Han, Q. M. Zhang and M. J. Serpe, *Nanoscale*, 2015, **7**, 2784–2789.
43 C. T. Greco, J. C. Andrechak, T. H. Epps and M. O. Sullivan, *Biomacromolecules*, 2017, **18**, 1814–1824.
44 J. He, P. Xiao, J. W. Shi, Y. Liang, W. Lu, Y. S. Chen, W. Q. Wang, P. Theato, S. W. Kuo and T. Chen, *Chem. Mater.*, 2018, **30**, 4343–4354.
45 A. Koh, D. Kang, Y. Xue, S. Lee, R. M. Pielak, J. Kim, T. Hwang, S. Min, A. Banks, P. Bastien, M. C. Manco, L. Wang, K. R. Ammann, K. I. Jang, P. Won, S. Han,

R. Ghaffari, U. Paik, M. J. Slepian, G. Balooch, Y. Huang and J. A. Rogers, *Sci. Transl. Med.*, 2016, **8**, 366ra165.
46 M. Holzinger, A. Le Goff and S. Cosnier, *Front. Chem.*, 2014, **2**, 63.
47 H. Meng and G. Li, *Polymer*, 2013, **54**, 2199–2221.
48 J. Hu, H. Meng, G. Li and S. I. Ibekwe, *Smart Mater. Struct.*, 2012, **21**, 053001.
49 G. Qing, M. Li, L. Deng, Z. Lv, P. Ding and T. Sun, *Mini-Rev. Med. Chem.*, 2013, **13**, 1369–1380.
50 M. A. C. Stuart, W. T. Huck, J. Genzer, M. Müller, C. Ober, M. Stamm, G. B. Sukhorukov, I. Szleifer, V. V. Tsukruk and M. Urban, *Nat. Mater.*, 2010, **9**, 101–113.
51 W. Wu and S. Zhou, *Nano Rev.*, 2010, **1**, 5730.
52 X. Li, Y. Gao and M. J. Serpe, *Macromol. Rapid. Commun.*, 2015, **36**, 1382–1392.
53 W. Liu, W. Zhang, X. Yu, G. Zhang and Z. Su, *Polym. Chem.*, 2016, **7**, 5749–5762.
54 J. Cai, T. Chen, Y. Xu, S. Wei, W. Huang, R. Liu and J. Liu, *Biosens. Bioelectron.*, 2019, **124**, 15–24.
55 A. Ghimire, O. Zore, V. Thilakarathne, V. Briand, P. Lenehan, Y. Lei, R. Kasi and C. Kumar, *Sensors*, 2015, **15**, 23868–23885.
56 C. Li and S. Liu, *J. Mater. Chem.*, 2010, **20**, 10716–10723.
57 T. Chen, Y. Xu, Z. Peng, A. Li and J. Liu, *Anal. Chem.*, 2017, **89**, 2065–2072.
58 T. Tanaka and D. J. Fillmore, *J. Chem. Phys.*, 1979, **70**, 1214–1218.
59 K. S. Soni, S. S. Desale and T. K. Bronich, *J. Controlled Release*, 2016, **240**, 109–126.
60 X. Wan, H. Liu, S. Yao, T. Liu and Y. Yao, *Macromol. Rapid. Commun.*, 2014, **35**, 323–329.
61 M. P. Wickramathilaka and B. Y. Tao, *J. Biol. Eng.*, 2019, **13**, 63.
62 W. Li, J. Nie, R. Hu, R. Zhao, W. Zhu, X. Chen, D. Li, L. Wang and L. Hu, *Chem. Commun.*, 2019, **55**, 9614–9617.
63 M. Dimde, F. F. Sahle, V. Wycisk, D. Steinhilber, L. C. Camacho, K. Licha, J. Lademann and R. Haag, *Macromol. Biosci.*, 2017, **17**, 1600505.
64 W. Zhang, M. Wei, W. S. Carvalho and M. J. Serpe, *Anal. Chim. Acta*, 2018, **999**, 139–143.
65 M. R. Islam and M. J. Serpe, *Anal. Chim. Acta*, 2014, **843**, 83–88.
66 O. Korostynska, K. Arshak, E. Gill and A. Arshak, *Sensors*, 2007, **7**, 3027.
67 M. Zhu, D. Lu, S. Wu, Q. Lian, W. Wang, A. H. Milani, Z. Cui, N. T. Nguyen, M. Chen and L. A. Lyon, *ACS Macro Lett.*, 2017, **6**, 1245–1250.
68 B. D'Autréaux and M. B. Toledano, *Nat. Rev. Mol. Cell Biol.*, 2007, **8**, 813.
69 T. Finkel, *Curr. Opin. Cell Biol.*, 2003, **15**, 247–254.
70 H. M. Yang, J. Y. Teoh, G. H. Yim, Y. Park, Y. G. Kim, J. Kim and D. Yoo, *ACS Appl. Mater. Interfaces*, 2020, **12**, 5413–5419.
71 L. Hu, Y. Wan, Q. Zhang and M. J. Serpe, *Adv. Funct. Mater.*, 2020, **30**, 1903471.
72 D. J. Denmark, R. H. Hyde, C. Gladney, M.-H. Phan, K. S. Bisht, H. Srikanth, P. Mukherjee and S. Witanachchi, *Drug Delivery*, 2017, **24**, 1317–1324.
73 X. Liu, H. Guo and L. Zha, *Polym. Int.*, 2012, **61**, 1144–1150.
74 J. B. Vincent, *Nutr. Rev.*, 2000, **58**, 67–72.
75 H. Arakawa, R. Ahmad, M. Naoui and H.-A. Tajmir-Riahi, *J. Biol. Chem.*, 2000, **275**, 10150–10153.
76 C. Ghobril and M. Grinstaff, *Chem. Soc. Rev.*, 2015, **44**, 1820–1835.
77 P. M. Kharkar, K. L. Kiick and A. M. Kloxin, *Chem. Soc. Rev.*, 2013, **42**, 7335–7372.
78 Z. Zhu, Y. Zhai, Z. Li, P. Zhu, S. Mao, C. Zhu, D. Du, L. A. Belfiore, J. Tang and Y. Lin, *Mater. Today*, 2019, 52–79.
79 X. Lan, Z. M. Su, Y. D. Zhou, T. Meyer, Y. G. Ke, Q. B. Wang, W. Chiu, N. Liu, S. L. Zou, H. Yan and Y. Liu, *Angew. Chem., Int. Ed.*, 2017, **56**, 14632–14636.
80 Y. Chen, C. Zhang, L. Y. Li, C. C. Tuan, F. Wu, X. Chen, J. Gao, Y. Ding and C. P. Wong, *Nano Lett.*, 2017, **17**, 4304–4310.
81 Y. Ling, D. Zhang, X. Cui, M. Wei, T. Zhang, J. Wang, L. Xiao and Y. Xia, *Angew. Chem., Int. Ed.*, 2019, **58**, 10542–10546.
82 W. Lee, D. Kim, S. Lee, J. Park, S. Oh, G. Kim, J. Lim and J. Kim, *Nano Today*, 2018, **23**, 97–123.
83 B. Sierra-Martin and A. Fernandez-Barbero, *Adv. Colloid Interface Sci.*, 2016, **233**, 25–37.
84 W. P. Hall, S. N. Ngatia and R. P. Van Duyne, *J. Phys. Chem. C*, 2011, **115**, 1410–1414.
85 L. Y. Chen, C. M. Ou, W. Y. Chen, C. C. Huang and H. T. Chang, *ACS Appl. Mater. Interfaces*, 2013, **5**, 4383–4388.
86 T. Shu, Q. Shen, Y. Wan, W. Zhang, L. Su, X. Zhang and M. J. Serpe, *RSC Adv.*, 2018, **8**, 15567–15574.
87 H. Huang and M. J. Serpe, *J. Appl. Polym. Sci.*, 2015, **132**, 42106.
88 M. R. Islam, S. Xie, D. Huang, K. Smyth and M. J. Serpe, *Anal. Chim. Acta*, 2015, **898**, 101–108.
89 H. Chen, T. You, G. Xu, Y. Gao, C. Zhang, N. Yang and P. Yin, *Sci. China Mater.*, 2018, **61**, 1201–1208.
90 A. Sirelkhatim, S. Mahmud, A. Seeni, N. H. M. Kaus, L. C. Ann, S. K. M. Bakhori, H. Hasan and D. Mohamad, *Nanomicro Lett.*, 2015, **7**, 219–242.
91 J. W. Rasmussen, E. Martinez, P. Louka and D. G. Wingett, *Expert Opin. Drug Delivery*, 2010, **7**, 1063–1077.
92 W. Wu, S. Chen, Y. Hu and S. Zhou, *J. Diabetes Sci. Technol.*, 2012, **6**, 892–901.
93 J. Chen, H. M. Meng, Y. Tian, R. Yang, D. Du, Z. H. Li, L. B. Qu and Y. H. Lin, *Nanoscale Horiz.*, 2019, **4**, 321–338.
94 Y. Zhou, J. Cao, J. Zhao, Y. Xie, J. Fei and Y. Cai, *Microchim. Acta*, 2016, **183**, 2501–2508.
95 T. Shu, X. Lin, Z. Zhou, D. Zhao, F. Xue, F. Zeng, J. Wang, C. Wang, L. Su and X. Zhang, *Sens. Actuators, B*, 2019, **286**, 198–205.

96 L. Shang, J. Xu and G. U. Nienhaus, *Nano Today*, 2019, **28**, 100767.
97 S. Gou, Y. E. Shi, P. Li, H. Wang, T. Li, X. Zhuang, W. Li and Z. Wang, *ACS Appl. Mater. Interfaces*, 2019, **11**, 6561–6567.
98 J. H. Lü, Y. Q. Fu, D. M. Wang and C. L. Lü, *Sens. Actuators, B*, 2018, **254**, 996–1004.
99 X. Shen, X. Yang, C. Su, J. Yang, L. Zhang, B. Liu, S. Gao, F. Gai, Z. Shao and G. Gao, *J. Mater. Chem. C*, 2018, **6**, 2088–2094.
100 A. R. Petosa, D. P. Jaisi, I. R. Quevedo, M. Elimelech and N. Tufenkji, *Environ. Sci. Technol.*, 2010, **44**, 6532–6549.
101 C. Zhu, D. Du and Y. Lin, *Biosens. Bioelectron.*, 2017, **89**, 43–55.
102 K. Paek, H. Yang, J. Lee, J. Park and B. J. Kim, *ACS Nano*, 2014, **8**, 2848–2856.
103 W. Zhou, X. Gao, D. Liu and X. Chen, *Chem. Rev.*, 2015, **115**, 10575–10636.
104 S. K. Ghosh and T. Pal, *Chem. Rev.*, 2007, **107**, 4797–4862.
105 Y. Ma, K. Promthaveepong and N. Li, *Anal. Chem.*, 2016, **88**, 8289–8293.
106 S. Maji, B. Cesur, Z. Zhang, B. G. De Geest and R. Hoogenboom, *Polym. Chem.*, 2016, **7**, 1705–1710.
107 G. Bodelón, V. Montes-García, C. Fernández-López, I. Pastoriza-Santos, J. Pérez-Juste and L. M. Liz-Marzán, *Small*, 2015, **11**, 4149–4157.
108 J. Wang, Y. Wang, H. Chen, H. Xu, W. Wang and L. Bai, *Sens. Actuators, B*, 2018, **258**, 998–1007.
109 X. Zheng, L. Zhao, D. Wen, X. Wang, H. Yang, W. Feng and J. Kong, *Talanta*, 2020, **207**, 120290.
110 D. X. Wen, Q. R. Liu, L. Z. Li, H. X. Yang and J. M. Kong, *Sens. Actuators, B*, 2019, **295**, 40–48.